Computers and Concrete, *Vol. 19, No. 4 (2017) 347-356*
DOI: https://doi.org/10.12989/cac.2017.19.4.347

Using element-embedded rebar model in ANSYS for the study of reinforced and prestressed concrete structures

Bruna M. Lazzari*, Américo Campos Filho[a], Paula M. Lazzari[b] and Alexandre R. Pacheco[c]

Civil Engineering Graduate Program, Federal University of Rio Grande do Sul, 99 Oswaldo Aranha Ave, 90035-190, Porto Alegre, RS, Brazil

(Received July 22, 2016, Revised November 28, 2017, Accepted January 4, 2017)

Abstract. ANSYS is a software well accepted by professionals and academics, since it provides a variety of finite elements, material constitutive models, and linear and nonlinear analysis of structures in general. For the concrete material, for instance, the software uses an elastoplastic model with the Willam-Warnke surface of rupture (1975). However, this model is only available for finite elements that do not offer the possibility of use of the element-embedded model for rebars, demanding a much larger amount of elements to discretize structures, making numerical solutions less efficient. This study is, therefore, about the development of a computational model using the Finite Element Method via ANSYS platform for nonlinear analysis of reinforced and prestressed concrete beams under plane stress states. The most significant advantage of this implementation is the possibility of using the element-embedded rebar model in ANSYS with its 2D eight-node quadratic element PLANE183 for discretization of the concrete together with element REINF263 for discretization of rebars, stirrups, and cables, making the solutions faster and more efficient. For representation of the constitutive equations of the steel and the concrete, a proposed model was implemented with the help of the UPF customization tool (User Programmable Features) of ANSYS, where new subroutines written in FORTRAN were attached to the main program. The numerical results are compared with experimental values available in the technical literature to validate the proposed model, with satisfactory results being found.

Keywords: reinforced and prestressed concrete beams; element-embedded rebar model; ANSYS; UPF

1. Introduction

Due to its importance to the structural engineering field, reinforced and prestressed concrete structural elements have been object of permanent study. This is due to the extremely complex behavior of the structural concrete as a material that, once subjected to internal forces, presents a highly nonlinear response. This nonlinearity is caused, among other factors, by cracking and the difference between tension and compression strengths of concrete; by yielding of steel and crushing of concrete; and by time related phenomenons, such as creep and shrinkage of concrete, as well as relaxation of steel. The knowledge of mechanical behavior and stress distributions in structural elements subjected to a certain load combination is fundamental to carry out a safe and cost optimized design.

The Finite Element Method (FEM) has already shown to be a well stablished and worldwide-acknowledged tool due to its capabilities when analyzing complex structures. Among commercial FEM-based computational packages, ANSYS platform is one that can be surely highlighted. This package is an important tool for nonlinear analysis of concrete structures, being frequently used on studies in this line of research. It can be found in the last years, numerous studies on concrete structures using ANSYS, among which can be cited: Kazaz (2010), Bulut *et al*. (2011), Amiri *et al*. (2011), and Anil and Uyaroglu (2012).

Considering recent studies, the work by Demir and Husem (2015) can be highlighted, where different modeling methods in ANSYS were considered to simulate the bonding loss in reinforced concrete elements using FEM. Another work worth mentioning was carried out by Vasudevan and Kothandaraman (2015), where ANSYS was used to study the effects of bending strengthening of reinforced concrete beams using external bars with different anchorage conditions. In the same line of research, herein is presented a computational model using ANSYS that applies the element-embedded rebar model to simulate numerically reinforced and prestressed concrete beams under plane stress states. Through an elastoplastic formulation, a computational model has been developed to find the proper deformed state of structures.

The implementation of the proposed constitutive model has been carried out by using the UPF customization tool (User Programmable Features) of ANSYS. This tool allows users to write their own code routines to address the definition of a new material behavior, the creation of a special finite element of a particular contact model, or even the specification of a new failure criterion. The numerical model proposed in this study is based in the Finite Element Method and was written in FORTRAN programming

∗Corresponding author, Ph.D. Student
E-mail: bruna.ml@gmail.com
[a]Professor
E-mail: americo@ufrgs.br
[b]Ph.D. Student
E-mail: p.manica.lazzari@gmail.com
[c]Professor
E-mail: apacheco@ufrgs.br

ISSN: 1598-8198 (Print), 1598-818X (Online)

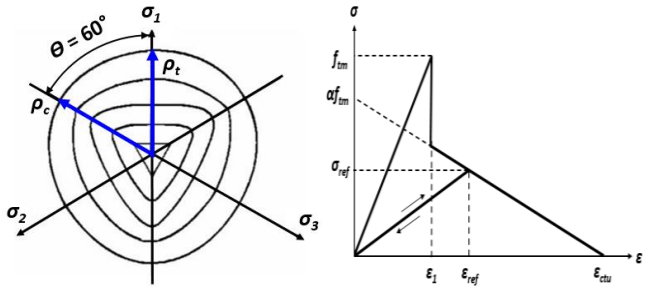

(a) Failure surface by Ottosen (1977) (b) Stress-strain curve for concrete under tension

Fig. 1 Criteria used to represent the behavior of concrete in compression and in tension

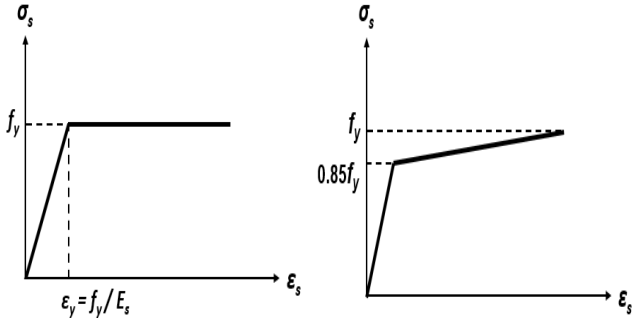

(a) Perfect elastoplastic model (b) Elastoplastic model with linear hardening

Fig. 2 Models used to represent steel behavior

language into the USERMAT routine (User Material Routine), which is present in the customization system of ANSYS. Regarding the used finite elements, 2D eight-node quadratic element PLANE183 with 2 degrees of freedom per node embedded with element REINF263 and the two-node linear element LINK180 have been selected for this study. In order to validate the implemented subroutines interfacing the main program (ANSYS), reinforced, pretensioned, and unbonded post-tensioned concrete beams that have been experimentally tested by Leonhardt and Walther (1962) and by Gongchen and Xuekang (1988) are numerically analyzed.

2. Material constitutive models

When analyzing the behavior of a structure, a deep knowledge of the mechanical properties as well as of the constitutive equations of the materials involved is fundamental. These constitutive equations are expressions that relate stresses, strains, and time, being essential in numerical simulations of a material such as the structural concrete, which is a blend of aggregates and cement paste associated with reinforcing bars and prestressing cables that together are strongly nonlinear.

2.1 Constitutive model for the concrete

Since concrete behavior is extremely complex, assembling its constitutive equations with consideration of all its material characteristics is not a simple task. For a situation where instantaneous loads are acting, and whether only instantaneous effects are wanted, an elastoplastic model should then be used up to reaching the failure surface of the material. Since the main characteristic of concrete is that it is a material with low tensile strength, relatively to its compressive strength, two different models to describe its behavior are used in this work. An elastoplastic model with hardening is used for the concrete under compression, while an elastic linear model is used for the concrete in tension, considering the contribution the concrete between cracks for the total stiffness of the structure.

The concrete model uses the failure criterion proposed by Ottosen (1977), which is the criterion suggested by *fib* Model Code (2012). It is admitted that the compressed concrete presents an elastoplastic behavior with isotropic hardening.

The concrete under tension, in its turn, is modeled as a linear elastic material with softening, i.e., before cracking occurs, the material behaves linear-elastically with softening and, after cracking, a smeared cracking model with tension stiffening is used. The cracking model used is based in the formulation presented by Hinton (1988). In Figs. 1(a)-(b) are represented the cross sections of the failure surface and the stress-strain diagram for the concrete under tension, respectively.

2.2 Constitutive model for the steel

Regarding the steel rebars and prestressing cables, it was considered that they would resist only to axial forces and present the same behavior when under tension or compression. The behavior is then given by a bilinear stress-strain diagram.

The steel rebars follow two behaviors, depending on the fabrication process of the material. When the material presents a yield plateau, a perfect elastoplastic model is adopted, but when cold rolled steel is considered, an elastoplastic behavior with linear hardening after 85% of the yielding stress, f_y, is used. In Figs. 2(a)-(b) are represented both the bilinear stress-strain diagram of the perfect elastoplastic model and the elastoplastic model with linear hardening.

However, particularly for post-tensioning steels, the behavior has been considered similar to that of cold rolled steel rebars, but being linear elastic up to 90% of the ultimate stress value. A linear behavior with hardening is considered after reaching this value.

3. Computational model

The Finite Element Method has been the method chosen to simulate numerically the reinforced and prestressed concrete structures of this study. With this method, the nonlinear behavior of the materials steel and concrete was possible to be considered, including processes such as concrete cracking and crushing, and steel plastification. ANSYS, in its version 14.5, was then used to create the

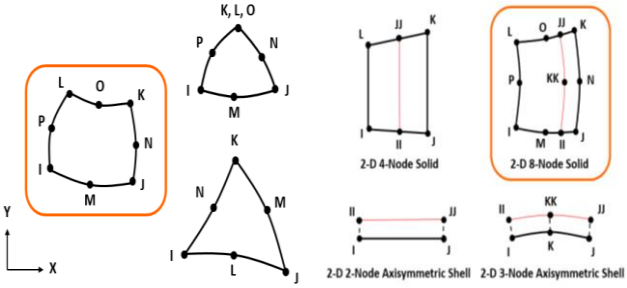

(a) Element PLANE183 (b) Element types that support element REINF263

Fig. 3 Finite elements used for concrete and steel discretization

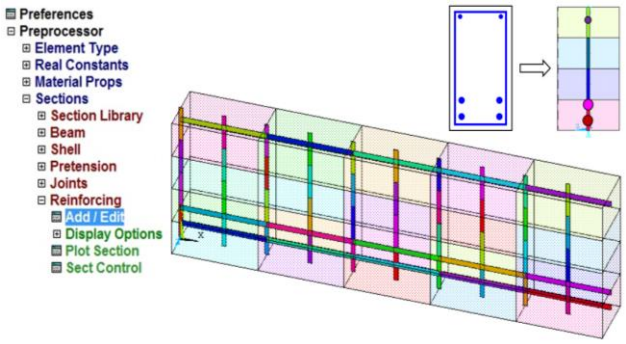

Fig. 4 Example of discretization with elements REINF263

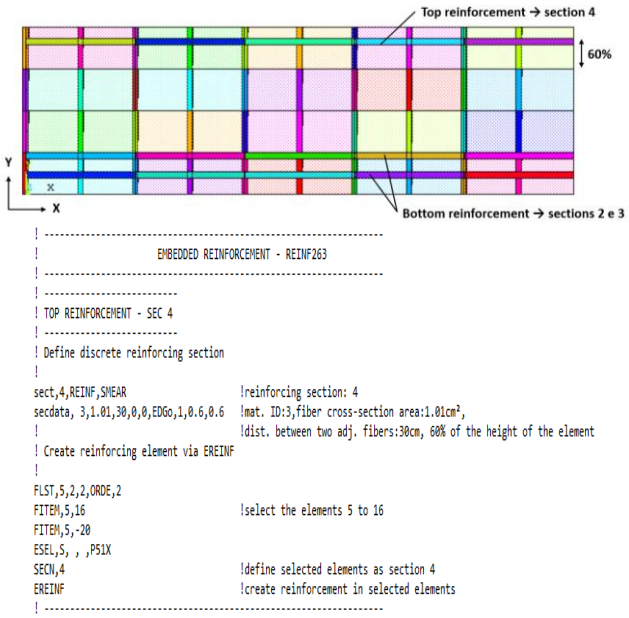

Fig. 5 Example of code scripting with elements REINF263 for top longitudinal rebars

numerical model proposed through UPF customization tool.

3.1 Types of finite elements used

The plane finite element PLANE183, which is in the list of elements of ANSYS library, was the element chosen to model the concrete regions of the structures studied. This is an element of higher order, quadratic, two-dimensional, with eight nodes with two degrees of freedom each, corresponding to translations in X and Y directions.

The plane stress case allows specification of a thickness for the element through ANSYS command "Real Constant". The element type PLANE183 has been chosen because it gives good results with relatively coarse meshes, significantly reducing the computational effort needed for the analysis. Besides, this element type has compatibility with element REINF263, which has been the element type used to model the reinforcing bars and stirrups.

The element REINF263, in its turn, can be used together with certain plane or shell elements of ANSYS library. This element is suited to simulate, for instance, reinforcing fibers aligned in one direction. In this case, each fiber could be individually modeled, taking into account material and cross section properties and considering only axial stiffness, and allowing the specification of many fibers into one basis element. The nodal coordinates, degrees of freedom, and connectivities of the reinforcing element are identical to those of the basis element. In the present study, this element was used to model both the rebars of the reinforced concrete beams, and the prestressing cables of the post-tensioned beams. The geometry of the element PLANE183 and of the finite element types that support element REINF263 are shown respectively in Figs. 3(a)-(b).

Since the basis for this study is the analysis of structural elements under plane state stresses, it was possible to lump together the rebars of the beams in the modeling, as can be seeen in Fig. 4. The same illustration also shows how to add the rebars via main menu as well as shows an example of beam discretization with transparency, allowing visualization of the REINF263 elements. However, code scripting is the more efficient method to add those elements, since it gets easier to verify possible mistakes. Fig. 5 presents an example of implementation of the top longitudinal rebars of beam ET1, which was originally tested by Leonhardt and Walther (1962), with element REINF263.

The use of the element REINF263 to model the prestressing cables of the unbonded post-tensioned beams was not possible. In this case, in order to simulate the unbonding between steel and concrete, the element LINK180 had to be used, which is a unidimensional finite element with three degrees of freedom per node, i.e., X, Y, and Z translations. It is important to highlight that the use of such type of element typically demands much finer finite element meshes. This occurs because LINK180 elements demand a discrete type of modeling at the anchorage points of the cables, i.e., the nodes of the element LINK180 that represent the cables have to coincide with the nodes of the elements PLANE183 that represent the concrete.

3.2 Modeling the concrete

In addition to a great variety of finite elements, ANSYS presents also a number of constitutive models to describe the behavior of materials. For concrete, as an example, the program uses an elastoplastic model with the failure surface of five parameters given by Willam and Warnke (1975). Unfortunatelly, this model is only available for element

```
! ----------------------------
!  CONCRETE - USER - material 1
! ----------------------------
!
!Constitutive model of user material
!
tb,user,1,2,5                    ! Material ID:1, 2 temperatures, 5 constants (prop)
tbtemp,1.0                       ! First temperature
tbdata,1,2754.8,0.2,2.42,2,21.002  ! Tempearature: 1, E, poisson, fc, aggregate, loading step
!                                ! Aggreg. 1: basalt, 2: quartz, 3: limestone, 4: sandstone
tb,state,1,,9                    ! Define 9 state variables
!
! --------------------------
```

Fig. 6 Example of use of the USERMAT routine for concrete

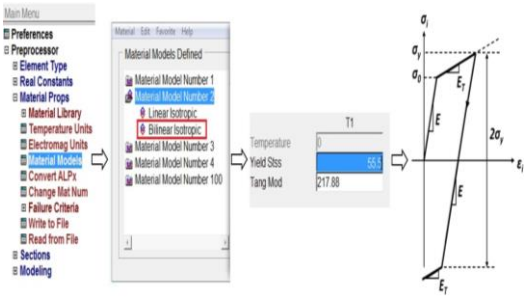

Fig. 7 The BISO model in ANSYS

SOLID65, which, in its turn, does not allow the use of the element-embedded type of modeling, demanding therefore a much larger amount of finite elements to model structures. Consequently, numerical simulations on structural concrete would become extremely slow, demanding machines with a much higher computational power.

With the objective of addopting the element-embedded model with elements REINF263 together with elements PLANE183, the customization tool UPF (User Programmable Features) of ANSYS had to be employed. Therefore, by using the UPF, it was possible to propose a new elastoplastic material model with cracking for the concrete and based on the failure criterion given by Ottosen (1977), which is currently recommended in the Model Code *fib* 2010 (2012). This new model has been implemented with the use of the programing language FORTRAN via USERMAT (User Material routine), a routine present in ANSYS customization system.

In order to have UPF available, ANSYS must be installed with the option "ANSYS Customization Files" activated, automatically creating the folders "custom" and "customize" inside folder "C:\Program Files\ANSYS Inc\v145\ansys". After accomplishing this, it was possible to access the routine USERMAT to write the new constitutive equations for the material. More specifically, the new concrete model was created inside the subroutine USERMATPS, which is called by routine USERMAT when plane stress state elements are used.

Routine USERMAT contains three other editable subroutines: USERMAT3D, for either axysimetric or plane stress/strain elements; USERMATBM, for 3D BEAM elements; and USERMAT1D, for unidimensional elements. The USERMAT routine is not only available for PLANE183 elements, but for a series of elements such as LINK180, SHELL181, PLANE182, SOLID185, SOLID186, SOLID187, BEAM188, and BEAM189. It is also necessary to compile and link the customized routine (in this work, the routine that has the proposed concrete model) to the main program ANSYS, creating a Dynamic-Link Library (DLL).

The USERMAT routine is used in any analysis of ANSYS of the mechanical type, being called in every Newton-Raphson iteration. In the initial time step, ANSYS stores stresses, displacements, and the necessary variables that are updated at the end of the time step. The input parameters necessary for the new constitutive model to work are given in an input file with the command "TB, USER". In Fig. 6, it is presented an example on how to use the new concrete model with that command. It can be seen that it needs only five variables to work: the modulus of elasticity; the Poisson ratio; the compressive strength of concrete; the type of coarse aggregate; and the number of steps, being other parameters determined internally.

3.3 Modeling the steel

Due to the already mentioned advantages of using the element-embedded model to discretize rebars in computational simulations, this was the type adopted in most of the analysis carried out in this study. The exception is the unbonded post-tensioning cables, which follow a discrete type of discretization.

In this study, two different constitutive models were used for the steel. For the reinforcing bars and stirrups, the BISO model (Bilinear Isotropic Hardening) was used, a model available in the internal library of ANSYS, and, for the prestressed cables, a model created with the UPF system and USERMAT1D subroutine was used.

The bilinear constitutive model BISO, which was used for rebars and stirrups, is defined as shown in Fig. 7. The initial slope of the strain-stress curve is given by the modulus of elasticity of the material, E. After reaching the initial yielding stress, σ_0, the diagram continues along a line with a slope defined by the tangent modulus, E_T, which characterizes the hardening phase of the material. The tangent modulus cannot be neither lower than zero nor larger than the initial modulus of elasticity.

4. Comments and results

Aiming to verify the efficiency of the model proposed for nonlinear structural analysis of reinforced and prestressed concrete, comparisons between experimental and numerical analysis are presented in the continuation. Initially, a comparison between the results obtained with the proposed computational model for four reinforced concrete beams originally tested by Leonhardt and Walther (1962) are presented. In the sequence, numerical results obtained with the model are compared with the experimental results carried out originally by Gongchen and Xuekang (1988), which were obtained with pretensioned and unbonded post-tensioned beams.

4.1 Leonhardt and Walther beams

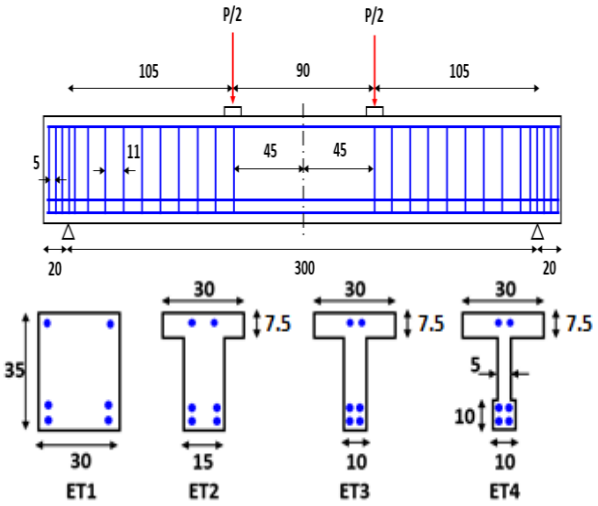

Fig. 8 Sketch of the longitudinal and cross sections of the beams tested by Leonhardt and Walther (1962) (dimensions in cm)

The study of a group of four simply supported reinforced concrete beams, identifyied as ET1, ET2, ET3, and ET4, tested by Leonhardt and Walther (1962) is presented in this item. In the tests, two concentrated loads were applied as shown in Fig. 8. These beams had the same span length of 3 m and the same height of 35 cm, but different cross sections. The compressive strength of the concrete was of 2.42 kN/cm^2. The longitudinal reinforcement was comprised of four rebars of 20 mm in diameter with yielding strength, f_y, of 42.8 kN/cm^2, being two placed 3 cm from the bottom of the cross sections and other two placed 6 cm from the bottom. Also comprising the longitudinal reinforcement, two rebars of 8 mm in diameter with yielding strength of 46.5 kN/cm^2, were placed 3 cm from the top of all cross sections. All longitudinal rebars were of the cold rolled (drawing) type of steel, a common type at the time of the experiments. The vertical stirrups were comprised of hot rolled rebars of 6 mm in diameter with yielding strength of 32 kN/cm^2, being distributed as shown in Fig. 8. The modulus of elasticity, E_s, of these steels were not reported, being considered in the numerical simulations to be as 210 GPa for the latter type of steel and 195 GPa for the former.

In order to study computationally these elements, geometrical and load symmetry were taking into consideration when modeling the beams with four elements in the height of their cross sections and five elements along their half spans. Therefore, a mesh of twenty 8-node quadratic quadrangular finite elements for plane stress states was adopted (PLANE183). Inside these elements, the elements REINF263 were then embedded to discretize the reinforcement of the beams. Fig. 9 presents an isometric view of the meshes used. Regarding the fixities, a roller in the Y direction was specified at the bottom node of the element at the end of the beams, with rollers in the X direction at each node located at the midspan cross section of the beams.

Just for the sake of comparison among quantities of finite elements used in the models, mesh distributions

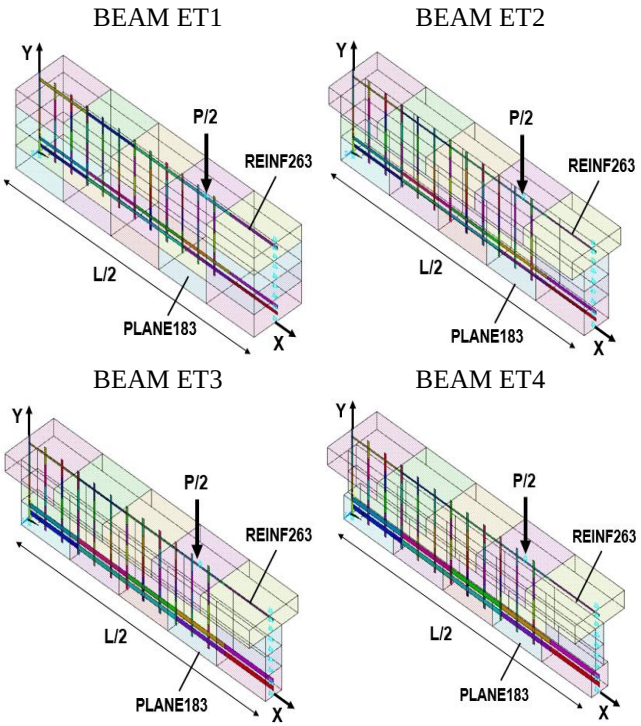

Fig. 9 Finite element discretrizations using the element-embedded rebar model for the beams tested by Leonhardt and Walther (1962)

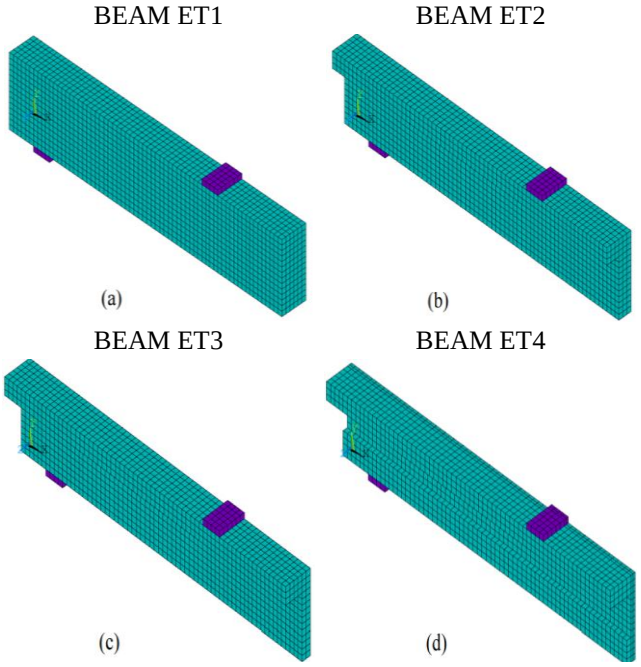

Fig. 10 Finite element discretrizations carried out by Kunzler (2013), using the discrete bar model for the beams tested by Leonhardt and Walther (1962)

carried out by Kunzler (2013) for the same beams by Leonhardt and Walter (1962), but using the discrete bar model for the reinforcement, are presented in Fig. 10. In these cases, only one fourth of the geometry of the beams was modeled, using SOLID65 elements to represent the concrete and LINK8 elements to represent the rebars. In the

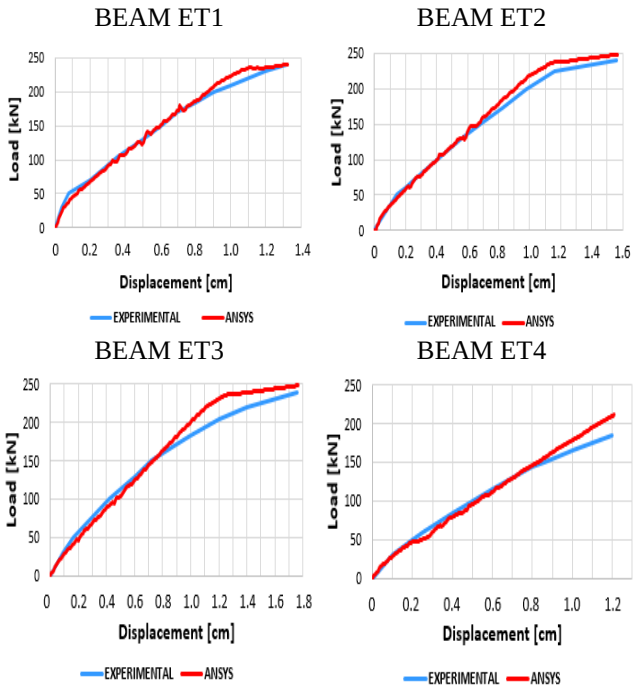

Fig. 11 Comparison between midspan displacements obtained from the experiments by Leonhardt and Walther (1962) and with the proposed model in ANSYS

computational analysis, for instance for beam ET1, 2.5 cm wide elements were considered, resulting in 5712 solid elements. Therefore, since only 20 elements are being used herein for the same case, this demonstrates and clarifies the computational gain obtained when the element-embedded rebar model is prefered instead of the discrete option.

The bilinear constitutive model BISO, which is available in ANSYS library, was used to discretize rebars and stirrups. As already mentioned, for the concrete, a new model implemented through the routine USERMAT was proposed. Then, load-displacement curves, deformed profiles, and stress diagrams for the concrete and reinforcement were calculated to validate the new model. Incidentally, since the own weight of the beams is too small in comparison with the applied loads, the analysis carried out do not considered such contribution.

In Fig. 11, it is possible to observe the load-displacement curves for beams ET1, ET2, ET3, and ET4, showing also their midspan deflection development with the applied load. The load was applied by imposing vertical displacements at the same location of the concentrated load to simulate an instantaneous loading case up to the collapse of the beams. Thus, the load axis of the load-displacement diagram was obtained by just multiplying the values of the vertical reactions of the beams by 2. The vertical displacements were measured at the bottom node of the cross section localized at the midspan of each beam. It can be seen from the results, that the load-displacement diagrams show a good correlation between the curves presented.

Figs. 12 to 15 show the calculated deformed profile of the beams originally tested by Leonhardt and Walther (1962) when rupture occurs, i.e., they show the maximum

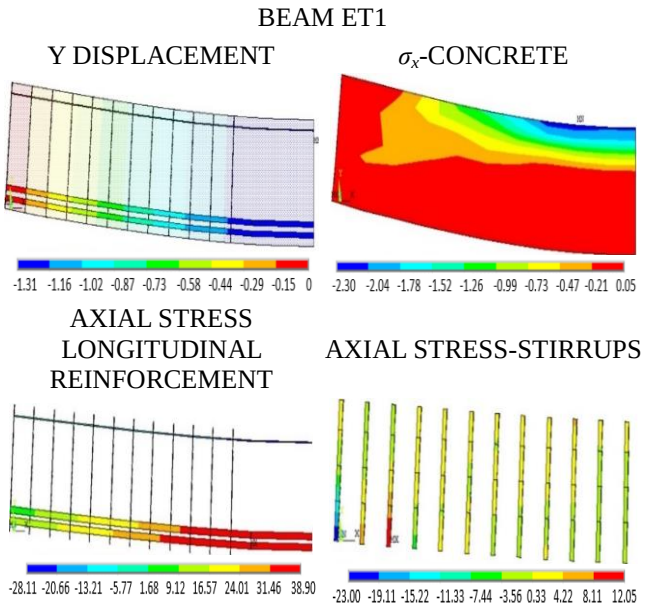

Fig. 12 Results obtained with the proposed model for beam ET1 originally tested by Leonhardt and Walther (1962)

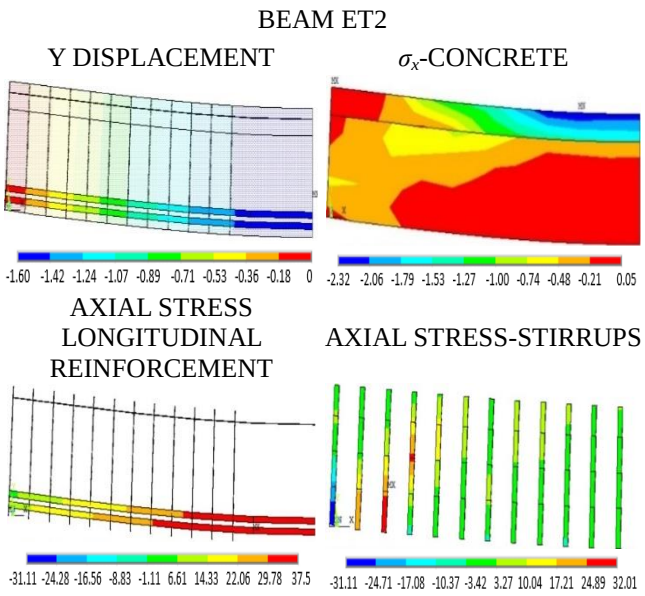

Fig. 13 Results obtained with the proposed model for beam ET2 originally tested by Leonhardt and Walther (1962)

midspan deflection reached by the structures just before their collapses. In order to observe better the stress distribution along the structures, the stresses are presented both in the concrete and in the reinforcement. It can be seen that, when the web width is reduced, decreasing the cross-sectional area of the beams, the stresses on the stirrups increase and shear collapse occurs.

In the diagrams of axial stresses, it can be observed that, for beam ET1, when the collapse load is reached, the bottom longitudinal reinforcement yields, but the stirrups are barely stressed. In both beams ET2 and ET3, it can be verified that the bottom rebars fall short to the yielding

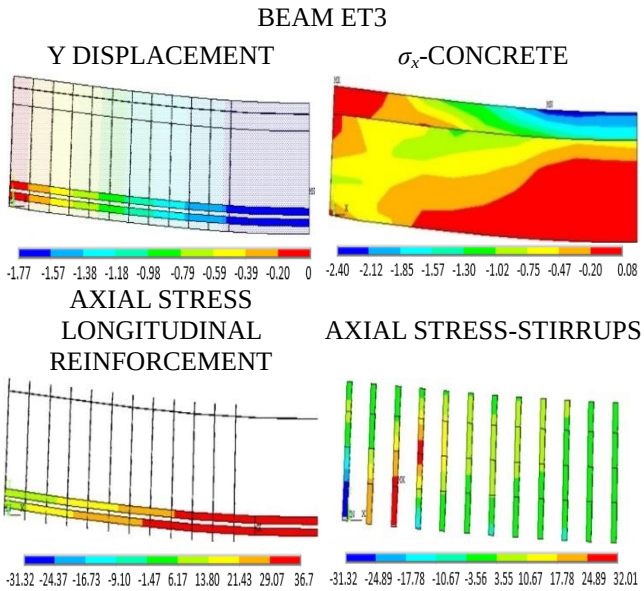

Fig. 14 Results obtained with the proposed model for beam ET3 originally tested by Leonhardt and Walther (1962)

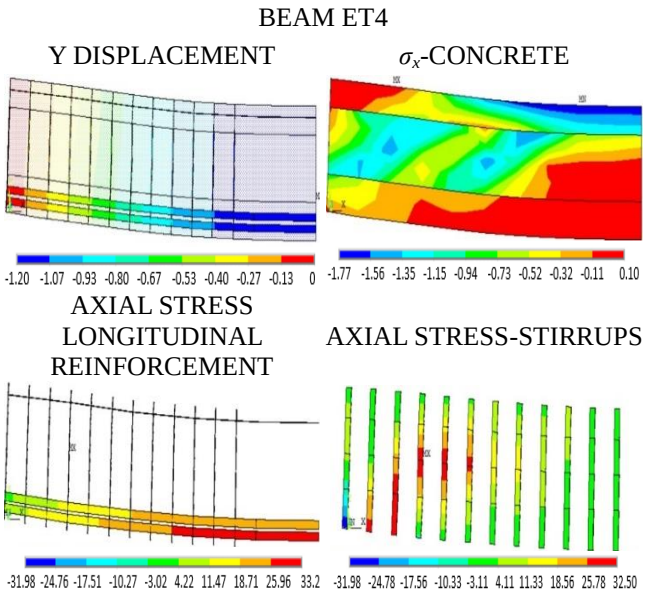

Fig. 15 Results obtained with the proposed model for beam ET4 originally tested by Leonhardt and Walther (1962)

stress, with stirrups reaching their maximum axial stress. However, beam ET4 reaches the maximum stress in the stirrups before yielding of the bottom reinforcement begins. Therefore, it becomes clear that beam ET1 collapses by bending, while beams ET2 and ET3 collapse by shear with an imminent rupture by bending, and beam ET4 collapses by shear.

4.2 Gongchen and Xuekang beams

In this item, it is presented the study of two simply supported prestressed concrete beams, one pretensioned and the other an unbonded post-tensioned beam that were originally tested experimentally by Gongchen and Xuekang (1988). For the pretensioned case, the bonding between concrete and steel was considered as perfect, i.e., with deformation compatibility between the nodes localized along the tendons and the nodes in the concrete. For the unbonded post-tensioned case, the tendons were only restrained to the concrete at some points along the span and at the anchorage points (ends of the beam). Therefore, the steel cables could move freely in relation to the concrete along the prestressing profile, with exception of those points cited, making the deformation compatibility hypothesis not valid for this case. Nevertheless, the main characteristic of structures with unbonded post-tensioning, when subjected to bending, is that the variation in length of the cables is equivalent to the variation in the total length of the structure, therefore guaranteeing a total displacement compatibility hypothesis. This results in a practically uniform distribution of stresses along the length of the unbonded cables, with these stresses being function of the average strain of the concrete along the cable profile.

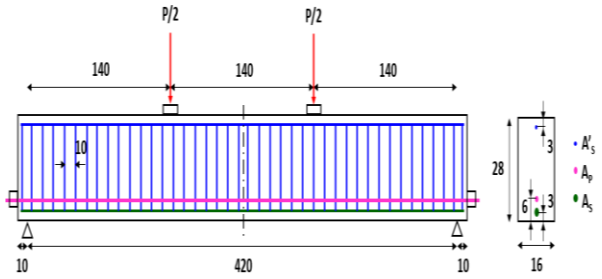

Fig. 16 Sketch of the longitudinal and cross sections of the beams originally tested by Gongchen and Xuekang (1988), (dimensions in cm)

Table 1 Characteristics of the beams tested by Gongchen and Xuekang (1988)

Beam	f_{cm} (kN/cm²)	A_P (cm²)	σ_{P0} (kN/cm²)	A_S (cm²)	f_Y (kN/cm²)	f_{ptk} (kN/cm²)	E_S (kN/cm²)	E_P (kN/cm²)
A-3	3.06	1.56	82	2.36	43	179	21000	20500
D-3	3.56	1.56	87.9	2.36	43	166	21000	20000

During prestressing of the cables and transfering of the prestressing forces to the anchorages, stress losses should occur, originated by mechanical causes such as friction along the cables and slippage of the anchorages. These losses, known as short-term or immediate losses, were not considered in the analysis carried out, only the ones known as long-term or time dependent losses, namely the relaxation of steel, and the shrinkage and creep of concrete were considered in this study.

Two models of beams with similar characteristics were analyzed to validate the model implemented into ANSYS, each with a particular prestressing condition: beam A-3 was unbonded post-tensioned, while beam D-3 was pretensioned. Both of them were subjected to two concentrated loads localized as illustrated in Fig. 16, i.e., similarly to the cases studied before. As can be seen, both beams had the same longitudinal reinforcing bars at the top of their cross sections, consisting of two bars of 6.3 mm of diameter, localized 3 cm from the top (A'_s=0.623 cm^2). The

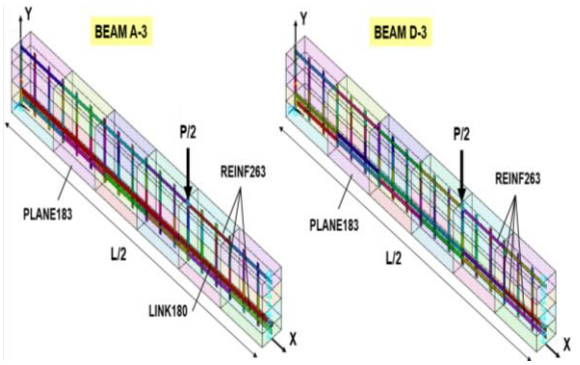

Fig. 17 Comparison between the discretization adopted for the reinforcing bars, stirrups, and prestressing cables for the beams tested by Gongchen and Xuekang (1988)

vertical stirrups were 6.3 mm in diameter and uniformly distributed by 10 cm apart. The following variables are given in Table 1 for each beam: average compressive strength of concrete, f_{cm}; cross-sectional areas of prestressing cables, A_p, and of bottom rebars, A_s; applied prestress, σ_{P0}; yielding stress of rebars, f_y; rupture stress of cables, f_{ptk}; modulus of elasticity of rebars, E_s and of cables, E_p (Gonghen and Xuekang 1988).

The numerical modeling of the two beams took advantage of their symmetry in both geometric and loading conditions, with the height of each one being divided into four finite elements and their half-span in six elements. It was adopted, therefore, a mesh of twenty-four quadrangular quadratic finite elements of eight nodes for plane stress states (PLANE183). Inside these elements, REINF263 elements were embedded to represent both the pretensioning cables, which were present in beam D-3, and the reinforcing bars of both beams. For beam A-3, in order to represent better the unbonding between post-tensioning cables and the concrete matrix, only one element LINK180 was used, connected only at the ends of the beams. Fig. 17 presents an isometric view of the elements of ANSYS used in each case. Regarding external fixities, one roller was specified to restrict direction Y of the bottom node of the finite element at the end of the beams, while other rollers, restricting direction X, were specified to all nodes localized at the midspan cross sections.

Regarding the discretization of the longitudinal rebars and stirrups, a bilinear constitutive model BISO available in ANSYS library was used. The proposed model implemented through the USERMAT routine was used for the prestressing cables and the concrete.

The validation of the numerical analysis was carried out by evaluating load-displacement curves, deformed profiles of the structures, and the distribution of stresses in the concrete, rebars, stirrups, and cables. In these cases, their own weight was considered as a load of short-duration, since the experiments were carried out approximately 28 days after concrete pouring.

The values compared next are net values, i.e., the own weight contribution has already been subtracted from the results. Fig. 18 shows the results from the experiments and from the computational model proposed in ANSYS, presenting the development of the midspan deflections with

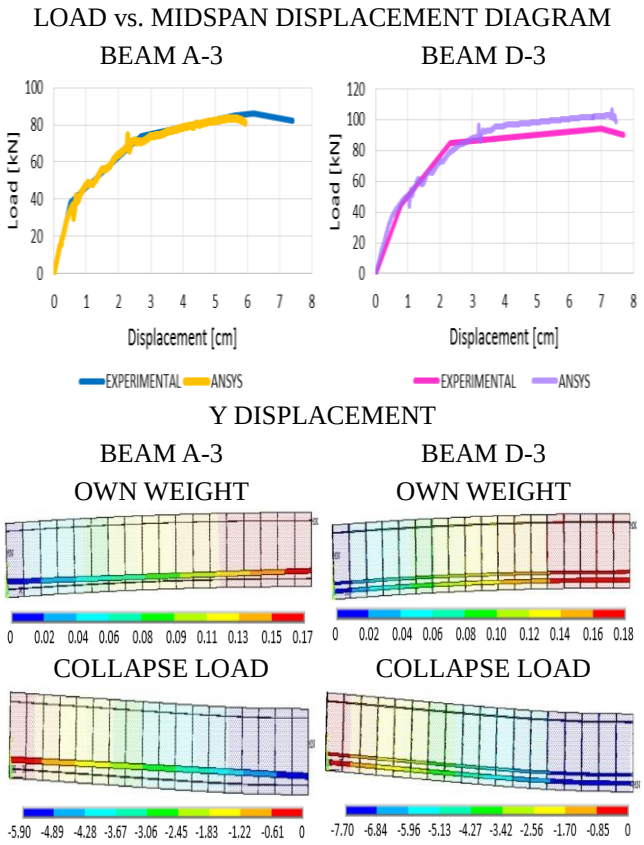

Fig. 18 Comparison between loads and midspan deflections obtained with the proposed model and experimentally by Gongchen and Xuekang (1988)

loading for both beams A-3 and D-3. As can be seen, the results in terms of load-displacement diagrams present a good correlation between the shown curves, also having a failure load value similar to that found experimentally.

Together with these curves, the deformed profiles of both beams A-3 and D-3 are also shown in Fig. 18 for the first load values, when the concrete had 28 days of age and the structures were subjected only to the prestressing force and their own weight, as well as for the ultimate load values, when collapse occurs. Based on these deformed profiles of the beams, it is possible to conclude that they present a negative midspan deflection initially, but the deflections become positive with loading increase, showing the effect of the prestress on the elements. It is interesting to observe that, for the unbonded post-tensioned beam A-3, there is no deformation compatibility, agreeing with the hyphothesis made initially, and that, except at the anchorages, the displacement of the finite element at the cables is independent of the displacement of the concrete finite elements. In the same way, analyzing the deformed profile of the prestressed beam D-3, it can be noticed that deformation compatibility do exists between steel and concrete finite elements, since the displacements of the prestressing cables follow the displacements of the concrete finite elements.

As can be seen in Fig. 18, the unbonded post-tensioned beam A-3 collapses under a lower load than the pretensioned beam D-3, also presenting a smaller midspan

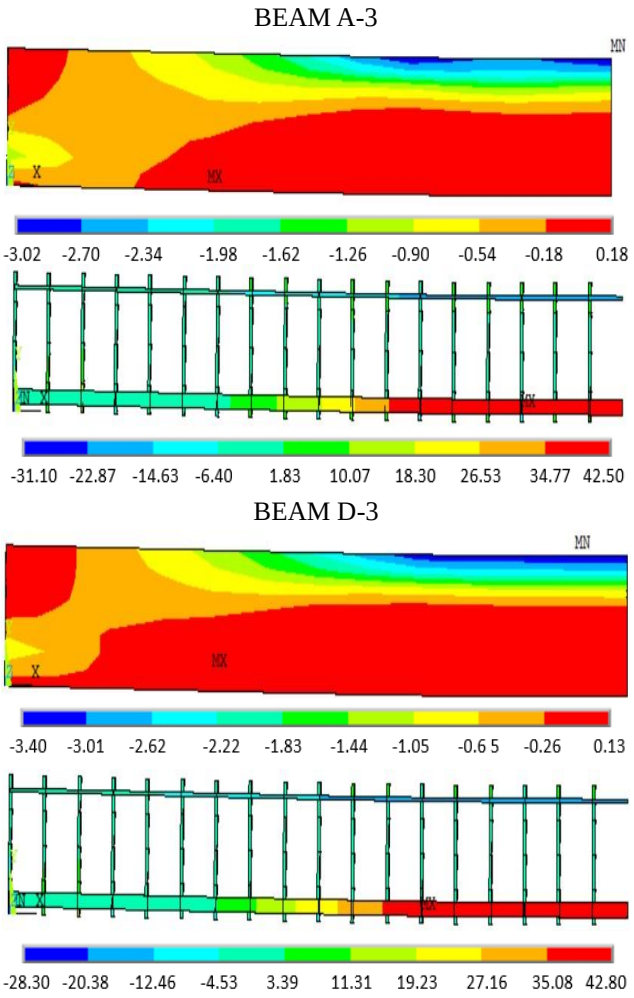

Fig. 19 Comparison between σ_x stresses in concrete elements and axial stresses in the reinforcing bars and stirrups of beams A-3 and D-3 for beams by Gongchen and Xuekang (1988)

deflection. This effect occurs because bonding has great influence in the cracking behavior of concrete, also changing the ultimate strength of prestressed beams. In beams with unbonded cables, for instance, the tendency is the formation of a small number of cracks with larger widths. However, in elements with bonded cables, which have a behavior similar to that of conventional reinforcement, there is the formation of a great number of cracks of smaller widths. Therefore, when transversal loads increase, cables suffer larger elongations in sections with opened cracks and, therefore, stresses in the steel increase considerably at these points, efficiently contributing to the resisting moment. In the case of unbonded cables, since the elongation due to localized crack openings dilutes along the cable length, the increases in stress are moderated and, consequently, the contribution to resisting moments is less efficient.

In Fig. 19 are presented, for the collapse condition, diagrams of σ_x stress distribution for the concrete elements, and diagrams of axial stresses for the reinforcing bars and stirrups for both beams A-3 and D-3, as obtained with the proposed model. It is possible to observe for both beams A-3 and D-3 that the bottom reinforcement is already yielding and higher compressive stresses are in the concrete, with stirrups being under little tension. It is also possible to observe the more elevated position of the neutral axis in the diagram of stress distribution in the concrete for both models.

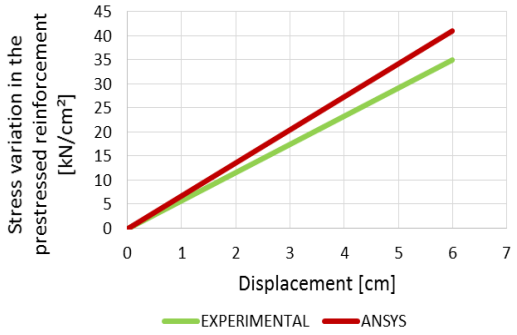

Fig. 20 Stress variation in the cables of beam A-3 calculated with the proposed model and measured experimentally by Gongchen and Xuekang (1988)

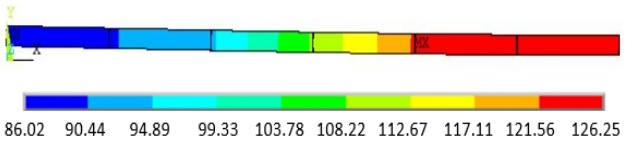

Fig. 21 Stress variation calculated with the proposed model in the cables of beam D-3, originally tested by Gongchen and Xuekang (1988)

Fig. 20 shows the development of the stress variation in the cables of beam A-3 with the midspan deflections, where can be seen the good agreement between the calculated results and the original experimental data. It is important to highlight that the axial stress obtained with the computational model along the cables of the unbonded post-tensioned beam is uniform along these cables for each loading displacement increment applied. It can be observed that the values calculated with the model are systematically a little higher than the values determined experimentally, but not affecting significantly the global behavior of the beams. This difference probably is due to the friction along the cables that was not considered in the model.

Fig. 21 presents the stress diagram for the cables of beam D-3 for the collapse condition as given by the analysis with the proposed model. It is worth mentioning that, contrary to what occurs with beam A-3, the axial stress obtained with the computational model for the pretensioned case varies along the cables with each displacement increment.

It is also worth mentioning that the prestressed beam D-3 was analysed using two different forms of discretization of the prestressing cables. In the first form, as already described, the element REINF263 was embedded in the concrete element. In the second form, the element LINK180 was connected to all nodes of the concrete elements to simulate bonding between the two materials steel and concrete. The results obtained after applying these two forms of modeling were rigorously identical. Nevertheless, the use of element REINF263 becomes more advantageous

than the use of element LINK180 because, with that choice, there is no need for a mesh discretization highly refined, optimizing the analysis. This advantage is particularly interesting for numerical simulation of prestressed beams with tendons of varied profiles, either curved or straight.

5. Conclusions

The study herein had the main objective of presenting an elastoplastic model based on the Finite Element Method to analyze numerically reinforced and prestressed concrete beams under plane state stresses. This model was developed in accordance with fib Model Code 2010 (2012) via programming language FORTRAN and was attached to the commercial software ANSYS through its USERMAT routine of the customization tool UPF. In this way, it was possible to generate in ANSYS a computational model that uses element-embedded rebars into concrete elements, reducing significantly the computational effort and making the modeling more versatile. ANSYS has shown to be a very suitable choice to implement the proposed model, since it has a large library of internally available finite elements, having also valuable tools for graphical visualization of results.

In order to validate the subroutines attached to the main program, four reinforced concrete beams originally tested by Leonhardt and Walther (1962) were analyzed herein, which are known cases in the literature that present a wide range of structural behavior, including collapses by bending and by shear. In the sequence, the efficiency of the computational model was again tested by analyzing the prestressed beams of both the pretensioned and the unbonded post-tensioned types that were originally tested by Gongchen and Xuekang (1988). Stresses in the concrete, rebars and tendons, deflected profiles, diagrams of load versus midspan deflections, collapse loads, as well as diagrams of deflections versus prestressing forces were analyzed herein. In accordance with the analysis carried out and the comparisons made herein between the numerical results and the experimental data, the model proposed has showed to be very realistic. Therefore, with the good results obtained with the model proposed, the possibility of simulating computationally the real behavior of more general structural concrete elements is quite promising. Additionally, it can be also highlighted that the UPF tool available in ANSYS allows structural analysis in a more efficient and precise fashion, with consequent optimization of materials.

A thorough analysis of the results, as well as more information regarding the models used and the scripts and codes written are presented in Lazzari (2015).

Acknowledgments

The authors wish to acknoledge the financial support given by the Civil Engineering Gratuate Program-PPGEC of the Federal University of Rio Grande do Sul-UFRGS, and by the Brazilian governmental research institutions CAPES and CNPq.

References

Amiri, G.G., Jahromi, A.J. and Mohebi, B. (2011), "Determination of plastic hinge properties for static nonlinear analysis of FRP-strengthened circular columns in bridges", *Comput. Concrete*, **10**(5), 435-455.

Anil, Ö. and Uyaroglu, B. (2012), "Nonlinear finite element analysis of loading transferred from column to socket base", *Comput. Concrete*, **11**(5), 475-492.

Bulut, N., Anil, Ö. and Belgin, Ç.M. (2011), "Nonlinear finite element analysis of RC beams strengthened with CFRP strip against shear", *Comput. Concrete*, **8**(6), 717-733.

Comité Euro-International du Béton (2012), CEB-FIP Model Code 2010, Bulletin N. 65.

Demir, S. and Husem, M. (2015), "Investigation of bond-slip modeling methods used in FE analyis of RC members", *Struct. Eng. Mech.*, **56**(2), 275-291.

Gongchen, D. and Xuekang, T. (1988), "Contrainte ultime dans câbles non-adhérents de poutres en béton a précontrainte partielle", *Annales de L'Institut Tecnhique du Batiment et des Tavaux Publics*, **462**, 75-88.

Hinton, E. (1988), *Numerical Methods and Software for Dynamic Analysis of Plates and Shells*, Pineridge Press Limited, Swansea, Wales, U.K.

Kazaz, I. (2010), "Finite element analysis of shear-critical reinforced concrete walls", *Comput. Concrete*, **8**(3), 143-162.

Kunzler, P.S. (2013), "Parametric analysis using the finite element method of reinforced concrete beams and presstressed concrete beams with openings", M.S. Dissertation, Federal University of Rio Grande do Sul, Porto Alegre, Brazil.

Lazzari, B.M. (2015), "Finite element analysis of reinforced and prestressed concrete elements under plane stress states", M.S. Dissertation, Federal University of Rio Grande do Sul, Porto Alegre, Brazil.

Leonhardt, F. and Walther, R. (1962), "Beiträge zur behandlung der schubprobleme im stahlbetonbau", *Beton und Stahlbetonbau*, **57**(7), 161-173.

Ottosen, N.S. (1977), "A failure criterion for concrete", *J. Eng. Mech. Div.*, **103**(4), 527-535.

Vasudevan, G. and Kothandaraman, S. (2015), "RC beams retrofitted using external bars with additional anchorages-a finite element study", *Comput. Concrete*, **16**(3), 415-428.

Willam, K.J. and Warnke, E.P. (1975), "Constitutive models for the triaxial behavior of concrete", *Proceedings of the International Association of Bridge Structures*, **19**, 1-30.

CC